

See discussions, stats, and author profiles for this publication at: <https://www.researchgate.net/publication/386559756>

Deep Learning Technique for automatic Liver and Liver Tumor Segmentation in CT Images

Article in *Journal of Liver Transplantation* · December 2024

DOI: 10.1016/j.j.liver.2024.100251

CITATIONS

0

READS

19

6 authors, including:



Yashaswini Gowda
Dayananda Sagar Institutions

8 PUBLICATIONS 15 CITATIONS

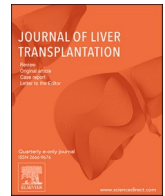
[SEE PROFILE](#)



Manjunath R V
Dayananda Sagar Academy of Technology and Management

8 PUBLICATIONS 97 CITATIONS

[SEE PROFILE](#)



Original article

Deep learning technique for automatic liver and liver tumor segmentation in CT images

Gowda N Yashaswini^a, R.V. Manjunath^{b,*}, B Shubha^c, Punya Prabha^d, N Aishwarya^a, H M Manu^b^a Department of Electronics & Communication Engineering, Dayananda Sagar College of Engineering, Bangalore-78, Karnataka, India^b Department of Electronics & Communication Engineering, Dayananda Sagar Academy of Technology and Management, Bangalore-82, Karnataka, India^c Department of Electronics & Communication Engineering, NMAM Institute of technology, Nitte, 574110, Karnataka, India^d Department of Electronics & Communication Engineering, Ramaiah Institute of technology, Bangalore, 560054, Karnataka, India

ARTICLE INFO

Keywords:

Computed tomography

Liver

Tumor

Semantic segmentation

128 × 128 size

UNet

ResUNet

Resnet,3D-IRCADb

Dice similarity coefficient

Precision

ABSTRACT

Segmenting the liver and tumors from computed tomography (CT) scans is crucial for medical studies utilizing machine and deep learning techniques. Semantic segmentation, a critical step in this process, is accomplished effectively using fully convolutional neural networks (CNNs). Most Popular networks like UNet and ResUNet leverage diverse resolution features through meticulous planning of convolutional layers and skip connections. This study introduces an automated system employing different convolutional layers that automatically extract features and preserve the spatial information of each feature. In this study, we employed both UNet and a modified Residual UNet on the 3Dircadb (3D Image Reconstruction for computer Assisted Diagnosis database) dataset to segment the liver and tumor. The ResUNet model achieved remarkable results with a Dice Similarity Coefficient of 91.44% for liver segmentation and 75.84% for tumor segmentation on 128 × 128 pixel images. These findings validate the effectiveness of the developed models. Notably both models exhibited excellent performance in tumor segmentation. The primary goal of this paper is to utilize deep learning algorithms for liver and tumor segmentation, assessing the model using metrics such as the Dice Similarity Coefficient, accuracy, and precision.

1. Introduction

The major organ in the human body is the liver which is prone to different malignant tumors leading to the death of millions of people around the globe. Liver tumor detection and its treatment to cure liver diseases has become a challenging point around the medical world. Identification of liver disease and proper treatment for the identified disease requires vital observation of the liver surface and its edges [1]. Best knowledge on the medical imaging techniques will allow to detect the liver diseases at a brisk space by the specialists. But there are lot of shortfalls like skilled specialists, low competency, high-cost labour in assessing the liver using best available medical imaging technology [2]. To identify liver lesions, we need to create a rigorous, effective, accurate and unbiased methods. Exciting research topic like semantic segmentation which can be used to label each pixel in an image and to differentiate the images into multiple components which gives diverse

behaviour and can solve high end visual problems. Due to the development of artificial intelligence and challenges like complex background, contrast variation, blurry edges, same pixel intensity of the neighbouring organs for the abdominal CT images made semantic segmentation [37] more exciting and attracting many scholars by providing various solutions.

Deep learning algorithms have significantly improved semantic segmentation in the twenty-first century, however even these algorithms are continually hampered by spatial anomalies. Chen et al. [3] enhanced the deep semantic pixel sorting model by incorporating a conditional random field, which improved the spatial uniformity of the segmentation results. Luc et al. [4] introduced a generative adversarial approach for training the segmentation model. Despite the low resolution of the feature map and the diverse appearances of entities in the image [39], the overall performance of the semantic segmentation was generally good and, in some cases, exceptionally accurate when using deep

* Corresponding author.

E-mail addresses: yashaswini-ec@dayanandasagar.edu (G.N. Yashaswini), manjunathrv@dsatm.edu.in (R.V. Manjunath), shubhab@nitte.edu.in (B. Shubha), punya.v@msrit.edu (P. Prabha), aishwaryan-ec@dayanandasagar.edu (N. Aishwarya), manu-ec@dsatm.edu.in (H.M. Manu).<https://doi.org/10.1016/j.liver.2024.100251>

Received 13 November 2024; Received in revised form 5 December 2024; Accepted 6 December 2024

Available online 8 December 2024

2666-9676/© 2024 The Author(s). Published by Elsevier Masson SAS. This is an open access article under the CC BY-NC license (<http://creativecommons.org/licenses/by-nc/4.0/>).

networks. To condense spatial irregularities and outcomes of the semantic segmentation a model consisting of encoder, decoder and a bridge is used. Here a hybrid model consisting of ResNet and UNet architectures are used which enhances the functioning of the model by surpassing current segmentation algorithms. The main highlights of the paper include.

1. The developed novel UNet and ResUNet models autonomously segment the liver and its tumors from the 3Dircadb dataset.
2. Tumor segmentation plays a crucial role in identifying various liver diseases.
3. A hybrid model was created by integrating residual blocks with the UNet architecture, enabling the extraction of deep features.
4. A specialized dataset was curated from the 3Dircadb (3D Image Reconstruction for computer Assisted Diagnosis database) dataset for experimentation.
5. The proposed ResUNet model demonstrated exceptional performance with Dice and precision values of **91.44%** and **84.42%** for the liver and **75.84%** and **62.41%** for liver tumors respectively using images sized at 128×128 pixels.
6. The proposed UNet model achieved a dice coefficient and Precision values of **91.27%**, **84.13%** for the liver and **73.50%**, **61.94%** for liver tumors with images sized at 128×128 pixels.
7. Based on the experimental findings it is evident that the hybrid ResUNet model outperforms UNet displaying the highest Dice Similarity Coefficient and excellent results in tumor segmentation.

The rest of the paper includes literature survey in [Section 2](#), methodology in [Section 3](#), [Section 4](#) results and analysis and [Section 5](#) conclusion.

2. Literature work

The medical filed provided a lot of opportunities for the researchers to find new ways to perform segmentation on CT images and to extract information from the segmented parts. The segmentation has its

applications in wide variety of fields such as face recognition, fingerprint recognition, disease identification etc. Below recent state of art methods is discussed.

Muazzam Maqsood et al. [5] developed a CAD system for effective liver tumor segmentation using residual learning combined with multi-scale parallel convolutions. This approach successfully segments tumors of different sizes directly from CT scans, addressing a challenging task of finding tiny tumors. The method leverages key residual connections to extract rich features while minimizing the number of parameters. The model evaluated on 3dircadb dataset which obtained a dice similarity coefficient of 77.15% and an accuracy of 93%. In future, performance of the model can be increased using attention gates.

Song Toan Tran et al. [6] introduced a novel approach named UNet for liver and tumor segmentation in CT scans, building upon the traditional UNet architecture with an n-fold network design. The UNet leverages convolution unit outputs at multiple layers, enhancing segmentation performance. The model was evaluated on publicly available datasets including LITS and 3Dircadb. On the 3Dircadb dataset, the model achieved a Dice Similarity Coefficient (DSC) of 96.45% for liver segmentation and 73.34% for liver tumor segmentation. Moreover, the versatility of this model extends to applications in positron emission tomography and ultrasound medical imaging.

Xiaomeng Li et al. [7] developed a unique segmentation model for identifying liver and tumors in CT scans, combining the strengths of 2D and 3D DenseUNet architectures. Their innovative H-DenseUNet model is designed to capture both detailed features within individual slices and the spatial relationships between slices. By integrating a fusion layer, the model effectively combines these intra-slice and inter-slice features, enhancing the learning process. The result is a highly accurate segmentation tool, achieving a Dice score of 98.2% for liver segmentation and 93.7% for tumor segmentation. Despite its impressive performance, the complexity of the model, with its 167 layers, means that training the network requires a significant investment of time.

Lu Meng et al. [8] developed a two-stage algorithm for liver and tumor segmentation utilizing convolutional neural networks (CNNs). The algorithm divides the task into two steps: first, performing liver localization, followed by tumor segmentation using CNNs enhanced with an attention mechanism to improve the segmentation of small liver tumors. The model's performance was evaluated on the LITS dataset, achieving Dice Similarity Coefficients (DSC) of 96.7% for liver segmentation and 72.5% for tumor segmentation. Future research will explore testing the model on diverse datasets to further validate its effectiveness.

Bo Wang et al. [9] introduced a method for accurate tumor segmentation using an Octave Convolutional Neural Network (Octave CNN). This approach leverages octave convolutions to learn multiple spatial frequency features, enhancing its ability to capture tumors of various sizes and shapes. Additionally, a deep supervision mechanism was incorporated during training to alleviate optimization challenges and enhance the model's discriminative capabilities. The proposed approach significantly outperformed the other methods in terms of accuracy, sensitivity, specificity, dice value and processing speed. Limitation of this approach is dataset as dataset requires manual labelling of liver diseases from an expert which is more time consuming and challenging task. In future, in this field 3D neural networks will be used for higher performance.

Xiaoling Xia et al. [10] introduced an enhanced 3D fully convolutional network that incorporates the squeeze-and-excitation method for liver segmentation. Here squeeze excitation method is used to adjust the input feature information. Using the improved feature calibration method, features related to liver are identified. This model is evaluated on two different datasets such as LITS and 3Dircadb for different metrics, where the model achieved a higher segmentation performance than any other models.

Patrick Ferdinand Christ et al. [11] employed two cascaded UNet models in their study on liver and liver lesion segmentation. One UNet

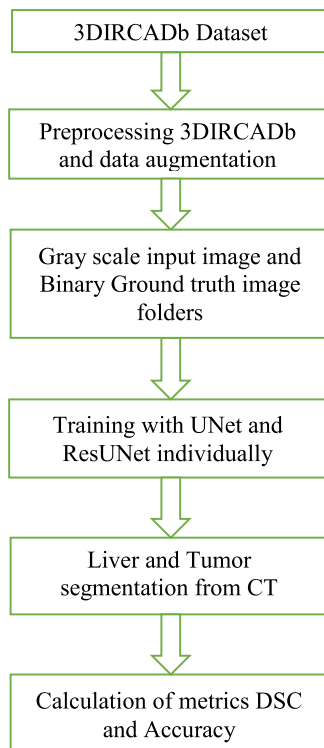


Fig. 1. Methodology flow chart

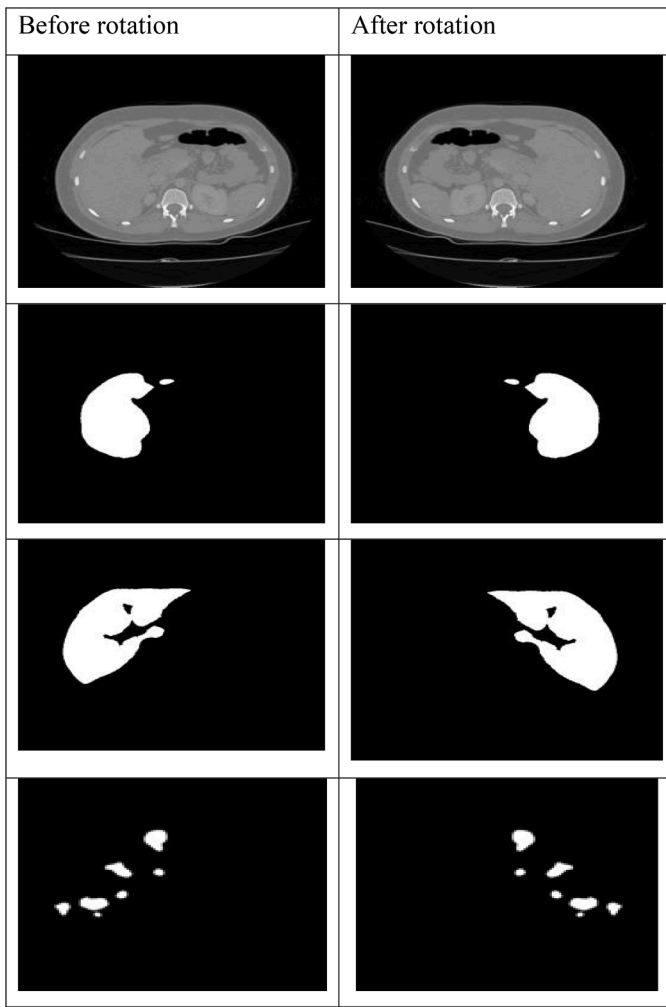


Fig. 2. 3Dircadb CT slices before and after rotation

model was dedicated exclusively to liver segmentation, while another focused-on tumor segmentation within a liver bounding box. The final segmentation result was further refined using a 3D conditional random field. The model achieved a Dice Similarity Coefficient (DSC) of 94%. Segmenting CT images of the liver and its tumors remains challenging due to their varied shapes and sizes, prompting significant research efforts to address these complexities.

3. Methodology

The 3DIRCADb dataset comprises of original 3D DICOM CT input images depicting various body organs such as liver, tumor, kidney, lungs, pancreas, etc., alongside their corresponding ground truths. For our study, we specifically focused on liver and tumor images from this diverse array of organs. Initially the 3D DICOM CT images of the liver and tumor from the 3Dircadb dataset were transformed into 2D JPG and PNG formats, adapting to our system's requirements. To optimize these images, they were scaled down to 0.25 and 0.50 from their original size of 512×512 . In our proposed methodology, we applied a modified Residual UNet and UNet on both the input images and their corresponding masks, employing various training configurations. Subsequently, the trained models underwent rigorous testing using a dedicated test dataset. The evaluation was based on key metrics such as the Dice Similarity Coefficient, Accuracy and Precision. The schematic representation of our structured framework is illustrated in Fig. 1.

3.1. Dataset and grouping

The 3DIRCADb [12] dataset, a widely accessible public resource, encompasses diverse organ data such as liver, liver tumors, kidney, spleen, and pancreas, among others. For our study we specifically focused on liver and tumor data from 20 patients aiming for precise liver and tumor segmentation. To facilitate effective training and testing we meticulously handpicked a total of 880 images ensuring the best quality and resized them to dimensions of 128×128 and 256×256 . In the preprocessing stage the original DICOM format images were converted into JPG and PNG formats. Additionally, these images were rescaled to 0.25 and 0.50 from their original size of 512×512 aligning them with our specific requirements. These images are processed and analysed using MATLAB 2023a software. To address the class imbalance between foreground and background we removed images lacking liver and tumor data from the dataset ensuring a more balanced representation. To augment the dataset and enhance the training process, we employed data augmentation techniques such as reflection and rotation. These techniques played a vital role in increasing the number of images compensating for the insufficient quantity of available data for robust training.

3.2. Data augmentation

Data augmentation is a crucial technique in biomedical image processing where datasets are often limited. It involves creating additional training and testing images by applying various transformations to the existing ones such as rotation, reflection and merging. These modifications help the network learn to recognize the same features despite different orientations or appearances enhancing its ability to generalize. In our case, we rotated the original CT images and their corresponding liver and tumor masks from the 3Dircadb dataset through various angles from 0 to 360° . This approach aims to prevent underfitting or overfitting by enriching the dataset with diverse examples as illustrated in Fig. 2 which compares the images before and after rotation.

3.3. Proposed architecture

The architectural designs of our models are represented as networks comprising distinct layers. The modified Residual UNet, a hybrid model combines the UNet architecture with two Resnet models. This innovative ResUNet [36] configuration incorporates 51 layers, encompassing encoder, decoder and bridge paths along with skip connections as depicted in Fig. 3(a). In contrast the UNet model comprises 49 layers including encoder, decoder and bridge paths but lacks skip connections as illustrated in Fig. 3(b). Throughout the training process detailed information about the network architecture including names, types, activations and learnable parameters is provided. Fig. 4(a) and Fig. 4(b) visually present the network layers of ResUNet and UNet respectively.

The developed novel hybrid model [42] for liver and tumor segmentation is created by integrating the foundational UNet architecture with ResNet resulting in a specialized system. Our model distinguishes itself with unique modifications and a departure from conventional approaches. Specifically, we implemented a 51-layer design without the typical batch normalization layer used for convolutional layer output normalization. Notably, during the expansion phase we introduced a maxpool layer after each convolutional and ReLU layer pair which greatly improved the model's performance. To address overfitting a dropout layer was strategically placed at the end of the encoder path to temporarily deactivate specific neurons.

The configuration of our model's convolutional blocks underwent meticulous adjustments. The initial block started with 32 filters progressively doubling in subsequent blocks and reaching a peak of 256 filters in the final convolutional block. The encoder responsible for feature extraction consisted of 8 convolutional layers followed by ReLU activation interspersed with 3 maxpooling layers and a dropout layer for

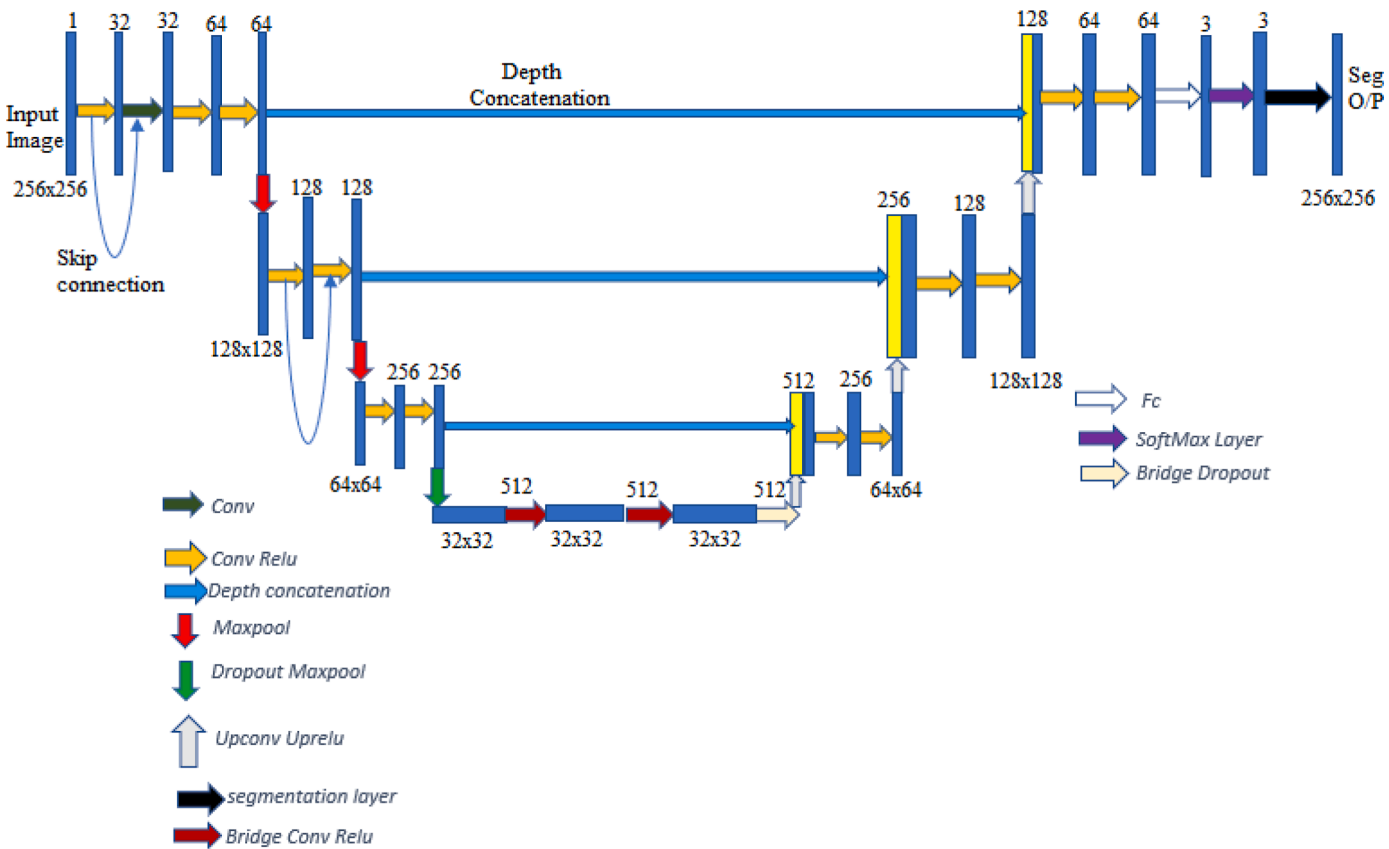


Fig 3a. ResUNet Architecture

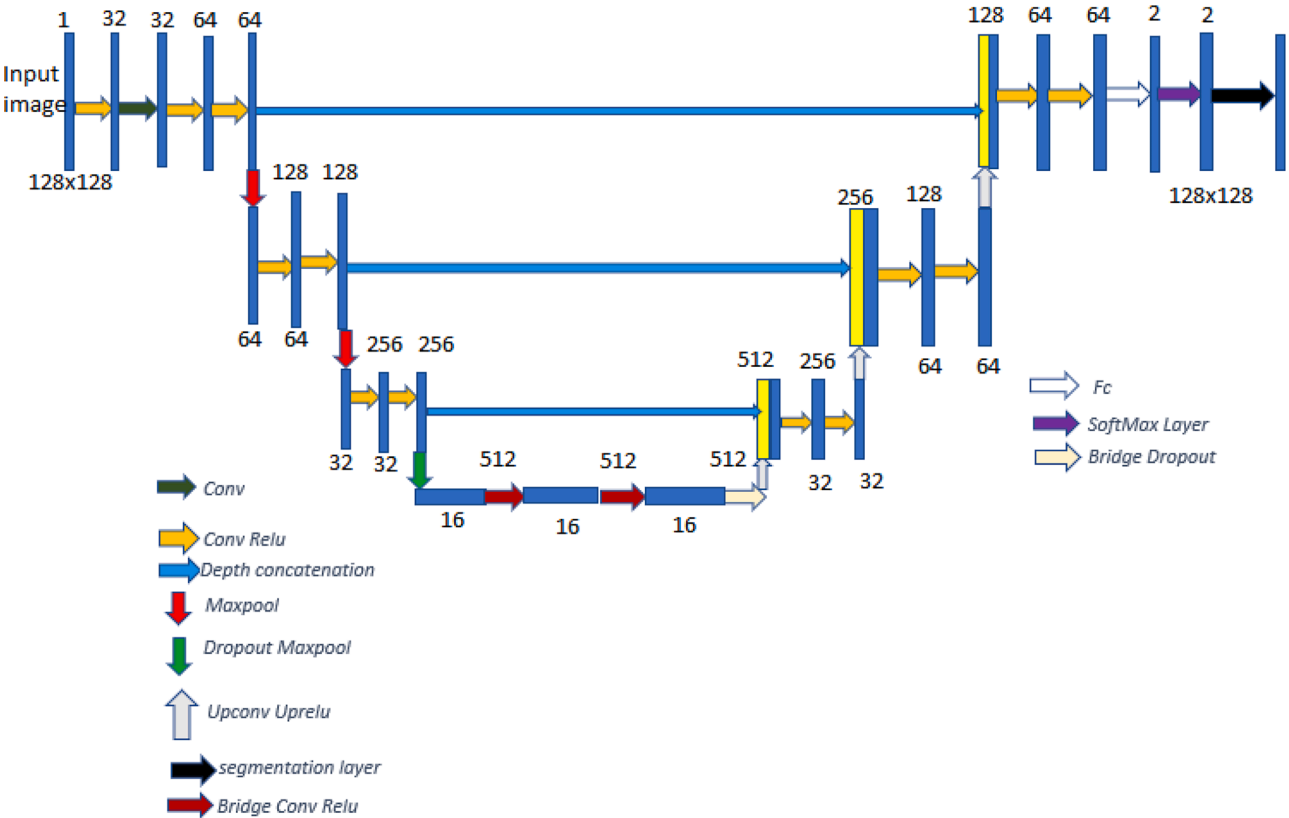


Fig 3b. UNet Architecture

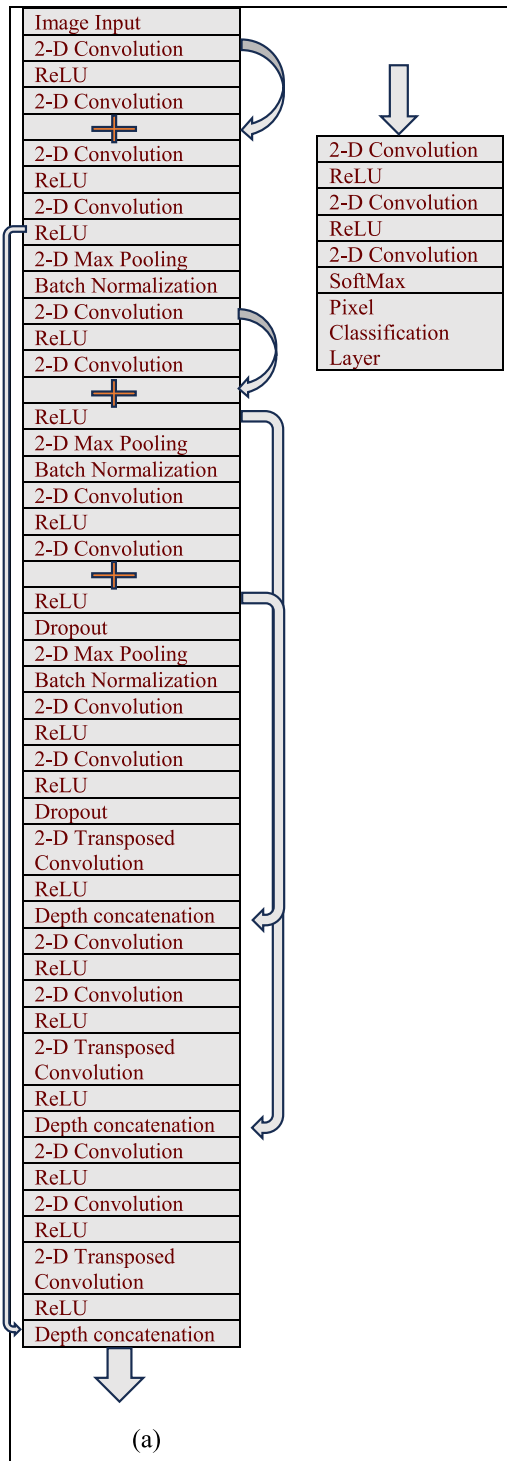


Fig 4(a). ResUNet Network Layers

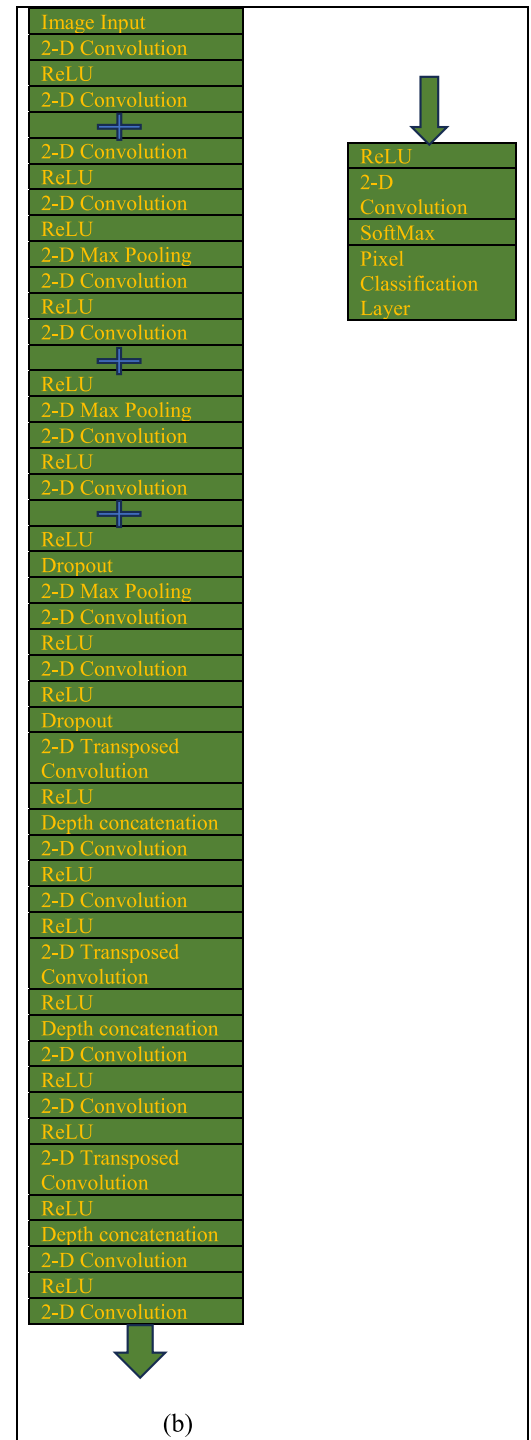


Fig 4(b). UNet Network Layers

regularization. Notably, we integrated two ResNet blocks within the encoder which played a crucial role in achieving precise segmentation of the liver and its tumors. On the decoder side we employed eight pairs of convolutional layers with ReLU activation complemented by four up convolution and upReLU layers strategically positioned. The smooth transition from the encoder to the decoder was facilitated by a bridge network that utilized four depth concatenation layers.

Several pivotal layers defined our architecture. The Convolutional Layer with a 3×3 filter computed dot products between filter weights and image content enabling feature extraction. The ReLU Layer as an

activation function eliminated negative values enhancing the model's non-linearity. The Maxpool Layer akin to convolutional layers selected maximum neighbouring values by reducing spatial size. A Dropout Layer was strategically placed to mitigate overfitting selectively deactivating neurons. The Depth Concatenation Layer seamlessly transferred features from the encoder to the decoder ensuring continuity in information flow. The Up Convolutional Layer employing transposed convolutions up-sampled output feature maps to restore spatial resolution. Furthermore, the model includes a Global Pooling Layer which evaluates the existence of features throughout the images offering a different approach compared to traditional fully connected layers. This layer is

strategically placed to enhance the model's ability to recognize patterns across various image inputs. At the final stage of the model a Fully Connected Layer serves as the decision-making component utilizing the features extracted during the learning process to make predictions. The SoftMax Layer which follows acts as the classifier assigning inputs to their respective categories based on the learned features. Lastly, the Classification Output Layer calculates the cross-entropy loss a critical function for weighted classification tasks ensuring that the model's predictions are as accurate as possible. These specialized layers contribute to the model's unique structure and its effectiveness in performing complex image segmentation tasks.

ResNet revolutionizes deep learning by introducing a core component known as the residual block which is pivotal in constructing deeper neural networks. Central to ResNet design is the implementation of skip connections which establish a direct link between the input and output of a block, evading some of the intermediate layers. This innovative approach effectively tackles the issue of vanishing gradients in deep networks as it allows gradients to flow more freely through these shortcut paths during backpropagation. Additionally, these skip connections empower ResNet to effectively learn the identity function meaning that the deeper layers can benefit directly from the features learned by the earlier layers thereby enhancing the network's overall efficiency and performance.

4. Results and discussions

This section contains subheadings explaining different segmentation assessing metrics as well as experimental results and their clarification.

4.1. Segmentation metrics

To assess the quality of segmentation metrics such as the Dice Similarity Coefficient (DSC) Accuracy and Precision are computed by comparing the original images with the segmented images.

1. **Dice Similarity Coefficient (DSC):** The Dice similarity coefficient quantifies the overlap between two binary images providing a measure of segmentation accuracy. A DSC value of 0 indicates complete segmentation failure while a value of 1 signifies perfect segmentation [13,14,41]. The following equation is used to calculate the Dice coefficient:

$$Dice(P, Q) = \frac{2|P \cap Q|}{|P| + |Q|} \quad (1)$$

2. **Accuracy:** Accuracy assesses the proportion of correctly identified pixels relative to the total number of pixels in the image. A perfect segmentation achieves an accuracy score of 1, whereas a score of 0 indicates no segmentation [15,38].

$$Accuracy = \frac{TN + TP}{TN + TP + FN + FP} \quad (2)$$

3. **Precision:** It is the ratio of correctly classified positive samples to the total number of classified positive samples [40].

$$Precision = \frac{TP}{TP + FP} \quad (3)$$

From all the above equations where P is the ground truth, Q is the Segmented output, TP represents True Positive, TN is True Negative, FP is False Positive, FN is False Negative and $|| = \text{Magnitude}$.

Table 1

Comparison of liver segmentation with state of art methods on 3Dircadb datasets size 128×128 .

Method	DSC (%)	Accuracy (%)	Precision (%)
Li W [16]	80.00	–	–
Yi Zhang [17]	91.00	–	–
Moghbel M [28]	91.10	–	–
Jeong J G [29]	89.90	–	–
Gibson E [30]	87.40	–	–
Rajamani K T [34]	90.75	–	–
Alom M [35]	90.81	–	–
Proposed method (UNet)	91.27	98.14	84.13
Proposed method (ResUNet)	91.44	98.18	84.42

Table 2

Comparison of tumor Segmentation with state of art methods on 3Dircadb datasets size 128×128 .

Method	DSC (%)	Accuracy (%)	Precision (%)
Yi Zhang [17]	56.70	–	–
Christ P F [18]	61.00	–	–
H Seo [19]	68.14	–	–
S T Tran [20]	73.34	–	–
Budak U [21]	63.40	–	–
Li X [22]	65.00	–	–
Karibasappa Kwadiki [23]	69.80	–	–
Jin Q [24]	59.50	–	–
Han X [25]	67.00	–	–
Ronneberger O [26]	67.50	–	–
Yodit A [27]	74.00	99.50	–
Song Toan Tran [31]	73.34	–	–
S Di [32]	71.00	–	–
B M Tummala [33]	72.00	–	–
Proposed method (UNet)	73.50	98.69	61.94
Proposed method (ResUNet)	75.84	98.70	62.41

4.2. Experimental results

The proposed method was implemented on a desktop computer using MATLAB version 2023a. The dataset was divided into training and testing sets with a ratio of 85% to 15%. The training was performed using a single central processing unit with parameter settings including a learning rate of 1×10^{-3} and a learning rate drop factor of 5×10^{-2} . The network underwent training for 200 epochs with each epoch consisting of 760 iterations resulting in a total of 1,52,000 iterations. The ResUNet employed 51 layers while the UNet utilized 49 layers during training. The comparisons between our proposed method and state-of-the-art approaches for 128×128 image sizes are presented in Tables 1 and 2 for liver and tumor segmentation respectively.

4.3. Liver segmentation

The metrics acquired for liver segmentation using the proposed ResUNet and UNet methods are presented in Table 1. Notably the ResUNet model outperformed UNet achieving outstanding segmentation results as showcased in Fig. 5. The results obtained for ResUNet include a Dice Similarity Coefficient of 91.44%, a precision of 84.42% and an accuracy of 98.18%. In Fig. 5 the top row illustrates the model outcomes where distinct colours represent different label IDs. The second row displays the segmented liver results while the third and fourth rows exhibit the original and input CT images respectively, utilized for testing purposes. This visualization provides a comprehensive view of the segmentation accuracy and highlights the ResUNet model's exceptional performance in liver segmentation.

4.4. Tumor segmentation

The metrics calculated for tumor segmentation are summarized in

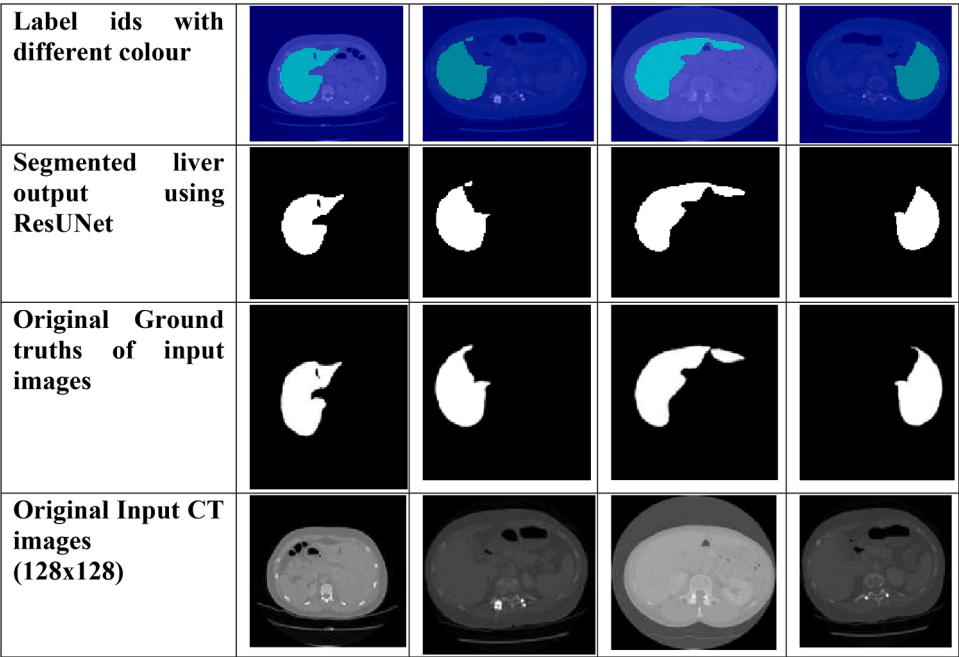


Fig. 5. Liver segmentation results of ResUNet

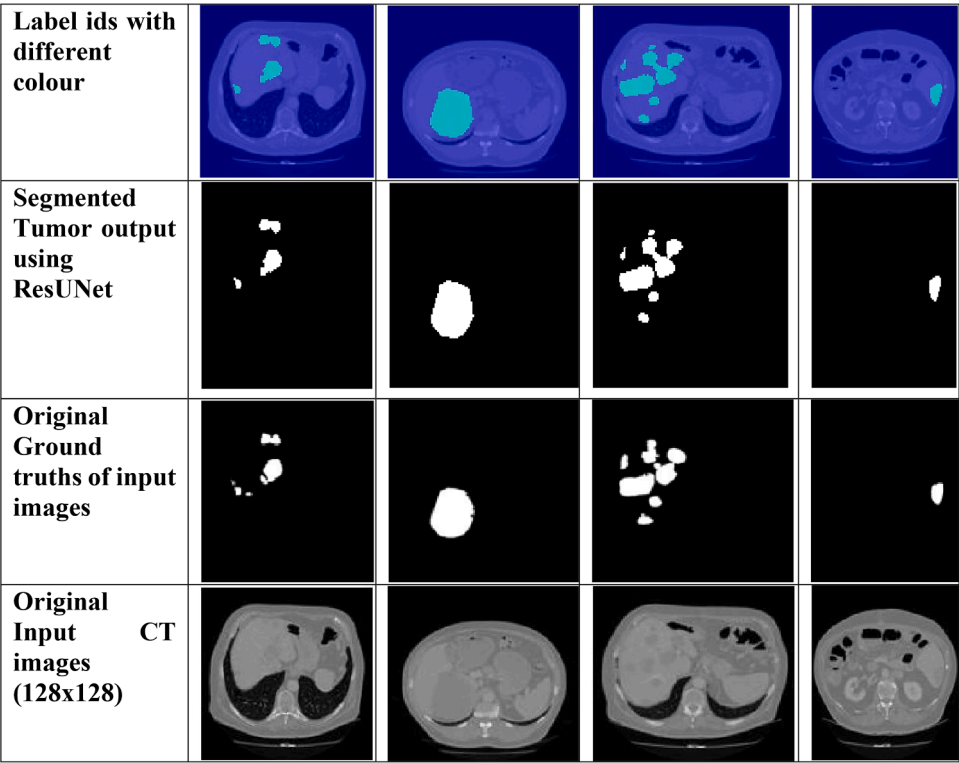


Fig. 6. Tumor segmentation results of ResUNet

Table 2 with the corresponding segmentation results illustrated in Fig. 6. ResUNet emerged as the superior performer in tumor segmentation achieving an impressive Dice Similarity Coefficient of 75.84%, a precision score of 62.41% and an accuracy of 98.70%. This exceptional performance surpassed that of UNet. In Fig. 6 the top row represents the model outcomes with distinct colours denoting different label IDs. The second row showcases the segmented tumor results while the third and fourth rows display the original and input CT images respectively. These

visual representations offer a clear depiction of the ResUNet model's superior accuracy in tumor segmentation, emphasizing its effectiveness in this critical medical application.

Figs. 7(a), 7(b) and 8(a), 8(b) illustrate the relationship between Accuracy vs Iterations and Loss vs Iterations respectively for the 3DIR-CADb tumor dataset over 200 training epochs. At the beginning accuracy increases whereas loss decreases across all the graphs. As the epochs approach the specified limit accuracy peaks while loss reaches its

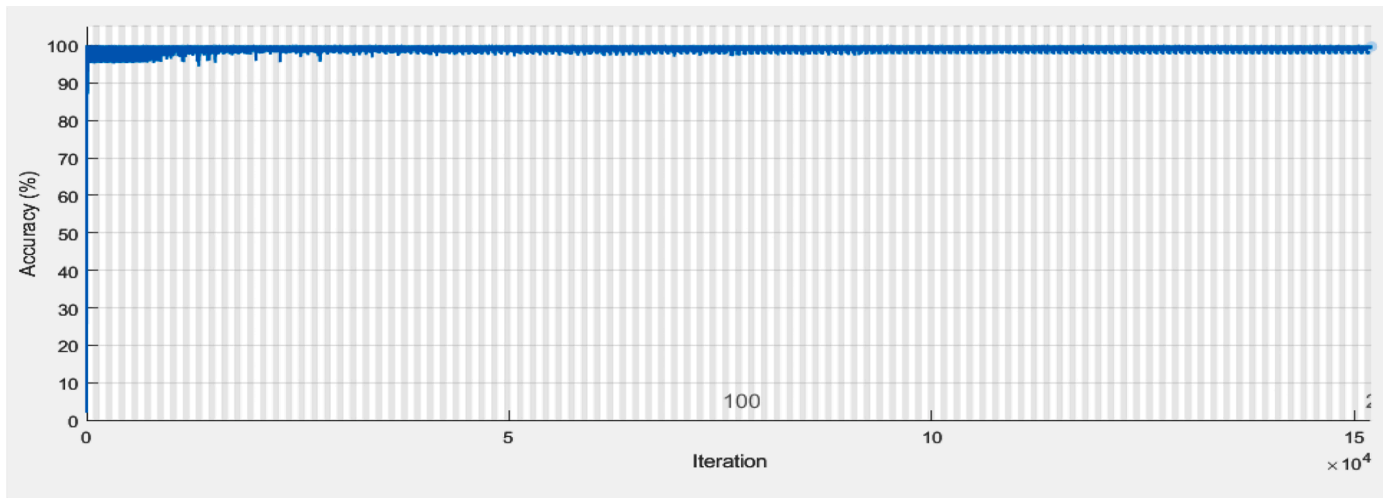


Fig. 7(a). Accuracy vs Iterations for UNet

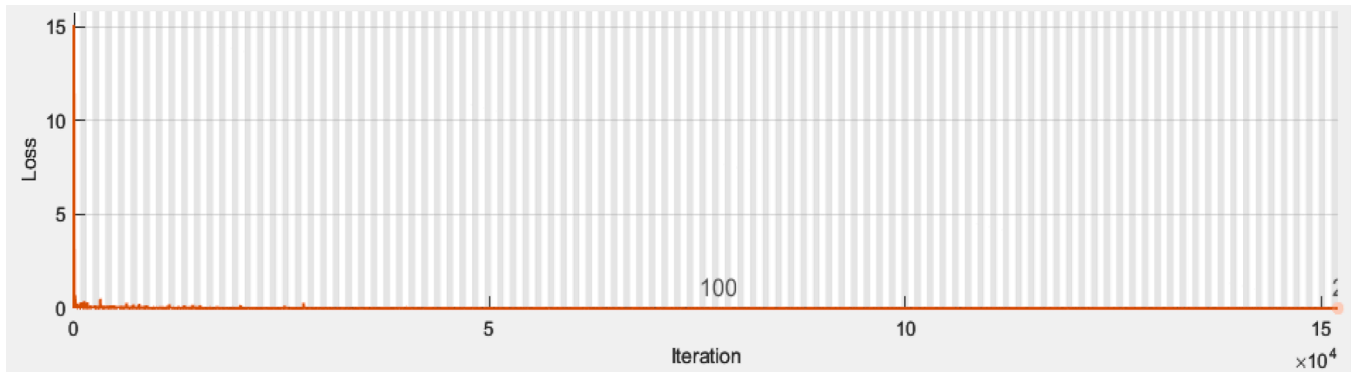


Fig. 7(b). Loss vs Iterations for UNet

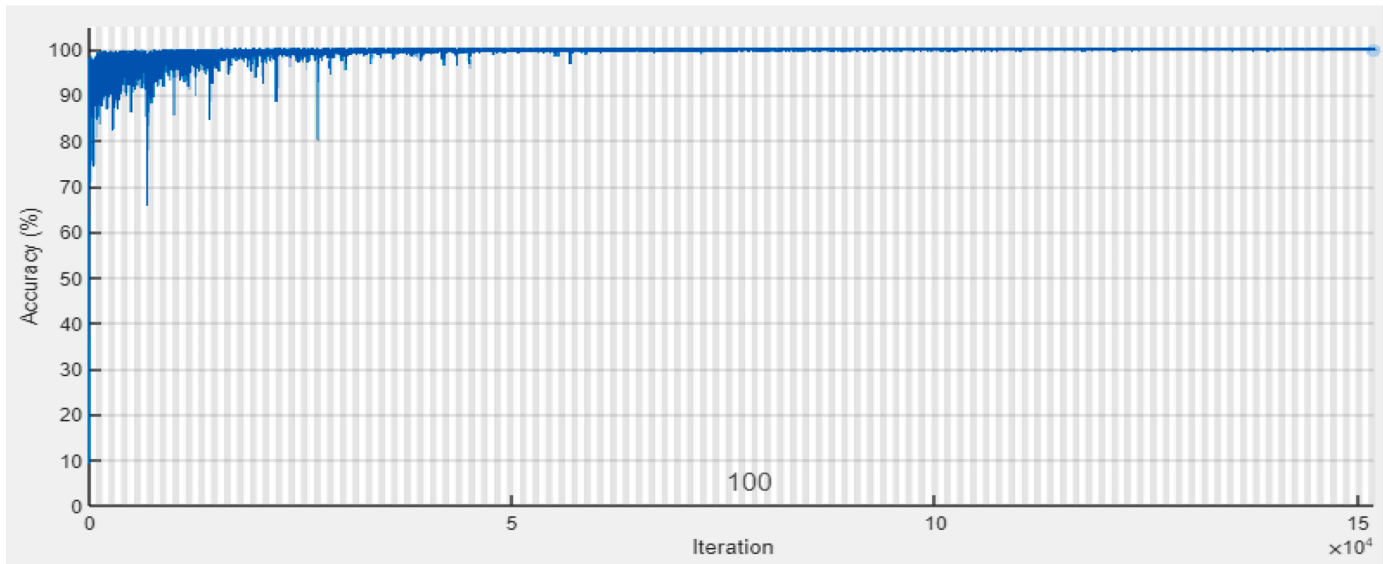


Fig. 8(a). Accuracy vs Iterations for ResUNet-51

lowest point. These graphical results confirm the model’s effectiveness in achieving the desired outcomes.

5. Conclusion

This paper explores liver and tumor segmentation using advanced deep learning algorithms applied to the 3Dircadb dataset. The study

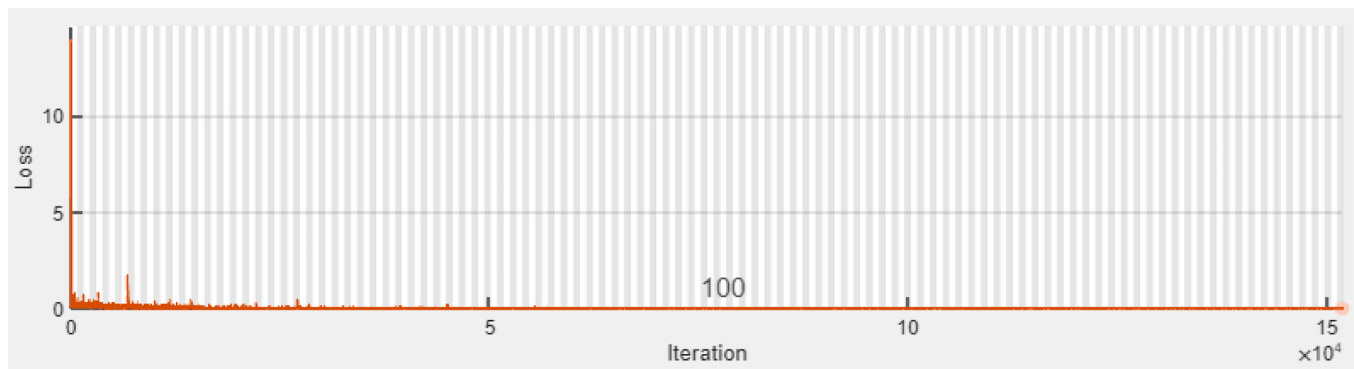


Fig. 8(b). Loss vs Iterations for ResUNet-51

specifically emphasizes the ResUNet model known for its effectiveness in tumor segmentation within CT images. A significant contribution of this research is the development of a modified ResUNet architecture which outperforms existing designs by achieving precise pixel-wise automatic tumor segmentation. The model demonstrates remarkable performance with a Dice Similarity Coefficient (DSC) of **75.84%**, Accuracy of **98.70%** and Precision score of **62.41%** for images sized at 128×128 pixels for tumor segmentation. Looking ahead the study aims to extend its scope to encompass various organ segmentations such as kidneys, pancreas and brain. Furthermore, efforts will be directed towards enhancing liver segmentation accuracy by meticulously fine-tuning different algorithmic parameters. Additionally, the research endeavours to explore diverse image sizes and conduct 3D liver volumetric analyses. This approach will facilitate a comprehensive assessment of liver health, aiding in the identification of different liver diseases. To bolster the model's robustness the study incorporates advanced pre and post-processing techniques. The research roadmap includes further experimentation with various convolutional neural network models on the different standard datasets to improve performance specifically in identifying even the smallest tumors.

Ethics approval and consent to participate

We comply to the ethical standards. We give our consent to participate.

Consent for publication

All the authors are giving consent to publish

Availability of data and materials

The datasets generated during and/or analyzed during the current study are available from the corresponding author on reasonable request.

Research involving human participation and/or animals

Not applicable

Informed consent

Not applicable.

Human and animal rights

The authors declare that the work described has not involved experimentation on humans or animals.

Informed consent and patient details

The authors declare that this report does not contain any personal information that could lead to the identification of the patient(s) and/or volunteers.

Funding

This work did not receive any grant from funding agencies in the public, commercial, or not-for-profit sectors.

Declaration of competing interest

No conflict of interest to declare.

References

- [1] Lu X, Xie Q, Zha Y, Wang D. Fully automatic liver segmentation combining multi-dimensional graph cut with shape information in 3D CT images". *Sci Rep* 2018;8 (3):10700–15.
- [2] Li X, Chen H, Qi X, Dou Q, Fu CW, Heng PA. 'H-DenseUNet: hybrid densely connected UNet for liver and tumor segmentation from CT volumes'. *IEEE Trans Med Imag Dec* 2018;37(12):2663–74.
- [3] Badrinarayanan V, Handa A, Cipolla R. SegNet: a deep convolutional encoder-decoder architecture for robust semantic pixel-wise labelling. *Comput Vis Pattern Recognit* 2015;32(3):1182–99.
- [4] P. Luc, C. Couprie, S. Chintala and J. Verbeek, "Semantic segmentation using adversarial networks", 2016, arXiv:1611.08408, [Online], Available: <https://arxiv.org/abs/1611.08408>.
- [5] Maqsood Muazzam, et al. A residual learning based multi-scale parallel convolutions assisted efficient cad system for liver tumor detection ". *Mathematics* 2021;9:1133. <https://doi.org/10.3390/math9101133>.
- [6] Tran Song Toan, et al. A multiple layer UNet UⁿNet, for liver and liver tumor segmentation in CT". *IEEE Access* 2021. <https://doi.org/10.1109/ACCESS.2020.3047861>.
- [7] Le Xiaomeng, a proposed, et al. Hybrid densely connected UNet for liver and tumor segmentation from CT volumes. *IEEE Trans Med Imaging* 2018;37(12). <https://doi.org/10.1109/TMI.2018.2845918>. December.
- [8] Meng Lu, et al. Two stage liver and tumor segmentation algorithm based on convolutional neural network". *Diagnostics* 2021;11:180. <https://doi.org/10.3390/diagnostics11101806>.
- [9] Wang Bo, et al. Accurate tumor segmentation via octave convolutional neural network. *Front Med (Lausanne)* 2021;8. <https://doi.org/10.3389/fmed.2021.653913>. May.
- [10] Xio Xiaoling, et al. Improved 3D fully convolutional network based on squeeze excitation method for liver segmentation. *Journal Physics* 2021. <https://doi.org/10.1088/1742-6596/2004/1/012007>.
- [11] Christ Patrick Ferdinand, et al. Automatic liver and lesion segmentation in ct using cascaded fully convolutional neural networks and 3D conditional random fields. Springer; 2016. p. 415–23.
- [12] Smeets D, Stijnen B, Loeckx D, Dobbelaer BD, Suetens P, Leuven KU. Segmentation of liver metastases using a level set method with spiral-scanning technique and supervised Fuzzy pixel classification. *3D Segment Clinic Grand Chall II-Liver Tumor Segmentation* 2008.
- [13] Bevilacqua V, et al. A novel approach for Hepatocellular Carcinoma detection and classification based on triphasic CT Protocol. A novel approach for hepatocellular carcinoma detection and classification based on triphasic ct protocol. 2017. p. 1856–63.
- [14] Ahmad M, et al. Deep belief network modelling for automatic liver segmentation. *IEEE Access* 2019;7:20585–95.

- [15] Zhang T, Zhang S, Jin C. A predictive model based on the gut microbiota improves the diagnostic effect in patients with cholangiocarcinoma. *Front Cell Infect Microbiol* 2021. <https://doi.org/10.3389/fcimb.2021.751795>. 2021.
- [16] Li W, Jia F, Hu Q. Automatic segmentation of liver tumor in CT images with deep convolutional neural networks. *J Comput Commun* 2015;3:146.
- [17] Yi Zhang, Xiwen Pan, Congsheng Li and Tonging Wu, "3D liver and tumor segmentation with CNNs based on region and distance metrics", *Appl Sci, MDPI*, doi:10.3390/app10113794.
- [18] Christ PF, Ettlinger F, Grun F, Elshaera MEA, Lipkova J, Schlecht S, Ahmaddy F, Tatavarty S, Bickel M, Bilic P. Automatic liver and tumor segmentation of CT and MRI volumes using cascaded fully convolutional neural networks. *ArXiv* 2017. arXiv:1702.05970.
- [19] Seo H, Huang C, Bassenne M, Xiao R, Xing L. Modified U-Net (mU-Net) with incorporation of object dependent high-level features for improved liver and liver-tumor segmentation in CT images. *IEEE Trans Med Imaging* 2020;39:1316–25.
- [20] Tran ST, Cheng CH, Liu DG. A multiple Layer U-Net, UnNet for liver and liver tumor segmentation in CT. *IEEE Access* 2021;9:3752–64.
- [21] Budak U, Guo Y, Tanyildiz E, Sengur A. Cascaded deep convolutional encoder-decoder neural network for efficient liver tumor segmentation. *Med Hypotheses* 2020;134:109431.
- [22] Li X, Chen H, Qi X, Dou Q, Fu CW, Heng PA. H Dense UNet: hybrid densely connected UNet for liver and tumor segmentation from CT volumes. *IEEE Trans. Med. Imaging* 2018;37:2663–74.
- [23] Manjunath RV, Kwadiki Karibasappa. Modified UNet on CT images for automatic segmentation of liver and its tumor. *Biomed Eng Adv, Elsevier* 2022. <https://doi.org/10.1016/j.bea.2022.100043>.
- [24] Jin Q, Meng Z, Sun C, Cui H, Su R. RA-UNet: a hybrid deep attention-aware network to extract liver and tumor in CT scans. *Front Bioeng Biotechnol* 2020: 1471.
- [25] Han X. Automatic liver lesion segmentation using a deep convolutional neural network method. *ArXiv* 2017. arXiv:1704.07239.
- [26] Ronneberger O, Fischer P, Brox T. U-Net: convolutional networks for biomedical image segmentation. In: *Proceedings of the International Conference on Medical Image Computing and Computer-Assisted Intervention*; 2015. p. 234–41. 5–9 October.
- [27] Ayalew YA, Fante KA, Mohammed MA. Modified U-Net for liver cancer segmentation from computed tomography images with a new class balancing method. *BMC Biomed Eng* 2021;3:4.
- [28] Moghbel M, Mashohor S, Mahmud R, Saripan MIB. Automatic liver segmentation on computed tomography using random walkers for treatment planning. *EXCLI J* 2016;15:500.
- [29] Jeong JG, Choi S, Kim YJ. Deep 3D attention CLSTM U-Net based automated liver segmentation and volumetry for the liver transplantation in abdominal CT volumes. *Sci Rep* 2022;12:6370. <https://doi.org/10.1038/s41598-022-09978-0>.
- [30] Gibson E, Giganti F, Hu Y. Automatic multi-organ segmentation on abdominal CT with dense V-networks. *IEEE Trans Med Imaging* 2018;37:1822–34. <https://doi.org/10.1109/TMI.2018.2806309>.
- [31] Tran ST, Cheng CH, Liu DG. A multiple layer U-Net, Un-Net, for liver and liver tumor segmentation in CT. *J Magazine, IEEE Access* 2020;9. <https://doi.org/10.1109/ACCESS.2020.3047861>. ISSN 2169-3536.
- [32] Di S, Zhao Y, Liao M, Yang Z, Zeng Y. Automatic liver tumor segmentation from CT images using hierarchical iterative super pixels and local statistical features. *Expert Syst Appl* 2022;203:117347.
- [33] Tummala BM, Barpanda SS. Liver tumor segmentation from computed tomography images using multiscale residual dilated encoder- decoder network. *Int J Imaging Syst Technol* 2022;32:600–13.
- [34] Rajamani KT, Siebert H, Heinrich MP. Dynamic deformable attention network (DDANet) for COVID-19 lesion semantic segmentation. *J Biomed Inf* 2021;119: 103816.
- [35] Alom M, Yakopcic C, Hasan M, Taha TM, Asari VK. Recurrent residual U-Net for medical image segmentation. *J Med Imaging (Bellingham)*. 2019;6(1):014006.
- [36] Manjunath RV, Yashaswini Gowda N. Automated approach for skin lesion segmentation utilizing a hybrid deep learning algorithm. *Multimed Tools Appl* 2023. <https://doi.org/10.1007/s11042-023-16934-1>. Springer.
- [37] Manjunath RV, Karibasappa K. Segmentation of CT images to extract liver using algorithms. *Int J Eng Adv Technol* 2020. <https://doi.org/10.35940/ijeat.C5827.029320>.
- [38] Manjunath RV, N Yashaswini Gowda, Manu HM, Lutimath Nagaraj M. Performance analysis of brain tumor classification on MRI images using pretrained deep learning models. *Res Sq* 2024. <https://doi.org/10.21203/rs.3.rs-3998886/v1>.
- [39] Manjunath RV. A few image processing algorithms on DM642. *Int J Trend Res Develop* 2019;6(4). ISSN:2394-9333.
- [40] Manjunath RV, Ghanshala Anshul, Kwadiki Karibasappa. Deep learning algorithm performance evaluation in detection and classification of liver disease using CT images. *Multimedia tools and applications*. Springer; 2023. <https://doi.org/10.1007/s11042-023-15627-z>.
- [41] Manjunath RV, Yashaswini Gowda N. Automated segmentation of liver tumors from computed tomographic scans. *J Liver Transplant* 2024. <https://doi.org/10.1016/j.liver.2024.100232>. Elsevier.
- [42] Yashaswini Gowda N, Lakshmikantha BR. On fly hybrid swarm optimization algorithms for clustering of streaming data. *Results in control and optimization*. Elsevier; 2023. <https://doi.org/10.1016/j.rico.2022.100190>.